07 - 10 September 2009

PROCEEDINGS

54. IWK

Internationales Wissenschaftliches Kolloquium

International Scientific Colloquium

Information Technology and Electrical Engineering - Devices and Systems, Materials and Technologies for the Future

Faculty of Electrical Engineering and Information Technology

Startseite / Index:
http://www.db-thueringen.de/servlets/DocumentServlet?id=14089

TECHNISCHE UNIVERSITÄT
ILMENAU

Impressum

Herausgeber:	Der Rektor der Technischen Universität Ilmenau Univ.-Prof. Dr. rer. nat. habil. Dr. h. c. Prof. h. c. Peter Scharff
Redaktion:	Referat Marketing Andrea Schneider Fakultät für Elektrotechnik und Informationstechnik Univ.-Prof. Dr.-Ing. Frank Berger
Redaktionsschluss:	17. August 2009

Technische Realisierung (USB-Flash-Ausgabe):
Institut für Medientechnik an der TU Ilmenau
Dipl.-Ing. Christian Weigel
Dipl.-Ing. Helge Drumm

Technische Realisierung (Online-Ausgabe):
Universitätsbibliothek Ilmenau
ilmedia
Postfach 10 05 65
98684 Ilmenau

Verlag: isle
Verlag ISLE, Betriebsstätte des ISLE e.V.
Werner-von-Siemens-Str. 16
98693 Ilmenau

ISBN (USB-Flash-Ausgabe): 978-3-938843-45-1
ISBN (Druckausgabe der Kurzfassungen): 978-3-938843-44-4

Startseite / Index:
http://www.db-thueringen.de/servlets/DocumentServlet?id=14089

LOCALIZATION OF AVALANCHE RESCUE TRANSCEIVERS BY MAGNETIC NEAR FIELD SIMULATION

Wolfgang Mayr [1] / Markus Stichler [1] / Gerd Waizmann [2]

[1] University of Applied Sciences Rosenheim, Hochschulstraße 1, 83024 Rosenheim
[2] proTime GmbH, Joseph-von-Fraunhofer Straße 9, 83209 Prien am Chiemsee

ABSTRACT

If a person is buried by an avalanche, the survivability decreases significantly within minutes [1]. Today skiers are usually equipped with standard avalanche rescue transceivers. After a signal from the buried transmitter is received (step 1), the rescuer follows the magnetic field lines towards the victim (step 2). However, in the most critical cases of deep burying the horizontal coordinates of the transmitter cannot be determined with the necessary precision by the standard method. So time consuming mechanical avalanche probing must be used for finally localizing the victim (step 3). We have developed a numerical technique for simulating the magnetic field of the transceiver based on some probes of the magnetic field vector. This enables us to calculate its horizontal position with an uncertainty of some cm. The latter two steps can therefore be combined, reducing the overall search time and complexity. This procedure has been successfully tested using an experimental setup consisting of a 3D – ferrite antenna and a USB data collection system connected to a laptop.

Index Terms – Avalanche rescue tranceiver, magnetic dipole field, near field simulation

1. INTRODUCTION

1.1. Standard Search Strategy

When localizing an avalanche victim the following standard search strategy is used. After the signal generated by the avalanche beacon of the victim is received for the first time from up to 50 m distance [2], the rescuer follows the magnetic field lines towards the victim on a bent path in that direction, where the signal strength increases. After crossing the victim's position the signal becomes weaker. The rescuer goes back to the position of maximum signal level and searches in the direction perpendicular to the first one for an even higher signal level. This procedure of alternating perpendicular search is repeated, until the position of maximum field level is localized (see figure 1). However, especially in cases of deep burying the precision of this method is not sufficient to start immediately to dig out the victim. So additional time consuming mechanical probing is necessary [3].

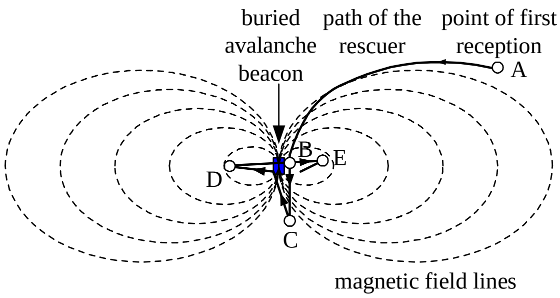

Figure 1 Standard Search Strategy
After the signal from the buried avalanche beacon has been received for the first time (point A), the rescuer goes towards the victim along the magnetic field lines generated by the buried avalanche beacon. At point B, he will get a maximum signal level (minimum distance display). He crosses this point until the signal becomes significantly weaker (point C) and turns round. Near the first maximum he tries to find a higher signal level by searching in the perpendicular direction (points D and E). However, the position of maximum signal level usually is not directly above the victim (see chapter 1.2), since the magnetic dipole antenna's direction is not defined. So time consuming mechanical probing is necessary before starting to dig out the victim.

1.2. Properties of the Magnetic Dipole Field

An avalanche beacon at the origin of the coordinate system generates an oscillating magnetic dipole field with a standard frequency of $457\,kHz \pm 80\,Hz$ [4]. In free space at the position $\vec{r}$ it can be written in real form and SI units as [5]

$$\vec{B}(\vec{r},t) = \frac{\mu_0}{4\pi}\cdot\left[3(\vec{n}\cdot\vec{m})\cdot\vec{n}-\vec{m}\right]\cdot\frac{1}{r^3}\cdot\cos(kr-\omega t) + \frac{\mu_0}{4\pi}\cdot\left[3(\vec{n}\cdot\vec{m})\cdot\vec{n}-\vec{m}\right]\cdot\frac{k}{r^2}\cdot\sin(kr-\omega t) + \frac{\mu_0}{4\pi}\cdot\left[(\vec{n}\times\vec{m})\times\vec{n}\right]\cdot\frac{k^2}{r}\cdot\cos(kr-\omega t) \qquad (1)$$

In this equation $\vec{m}$ denotes the vector of the magnetic dipole moment, $\vec{n}$ is a unit vector in the direction of $\vec{r}$ and $k = 2\pi/\lambda$ is the wave vector. The wavelength λ for 457 kHz is 656.5m. According to [10] at a distance of less than 4m used for the final search the free space solution for the magnetic field is adequate. The r – dependence of the three terms is $1/r^3$, k/r^2 and k^2/r, respectively. The first term in (1) describes the quasi - static B - field of a magnetic dipole with its $1/r^3$ dependence, the last one is the far field radiation term. The second term is an intermediate field contribution proportional to $1/r^2$. For a distance of $r = 1/k = 104.5m$ all three terms are of the same order, since the expressions in the squared brackets, describing the anisotropy of the field contributions, are all proportional to *m*. At a distance of e.g. 4m from the antenna the r-dependent terms have the ratio

$$1/r^3 : k/r^2 : k^2/r = 1 : kr : k^2r^2 = 1 : 0.038 : 0.0015\,.$$

The first and second term have the same anisotropy. Because of their time dependences $\cos(kr - \omega t)$ and $\sin(kr - \omega t)$, respectively, they have to be added in a RMS manner, so that a second term contribution of 3.8 % results in an amplitude change of $\sqrt{1 + 0.038^2} - 1 = 0.07\%$ only. From these considerations it becomes obvious, that for a maximum distance of 4m only the first term contributes within a measurement uncertainty of a few percent. Since the measurements for a precise localisation of the avalanche victim are made at distances of no more than 4m in the following we only consider the first term. This term is written as $\vec{B}_{QS}(\vec{r},t) = \vec{B}(\vec{r}) \cdot \cos(kr - \omega t)$, where $\vec{B}(\vec{r})$ is the magnetic flux density generated by a static magnetic dipole. $\vec{B}(\vec{r})$ is symmetric with respect to the axis of the ferrite antenna of the avalanche beacon defined by its magnetic moment $\vec{m}$. The equation for $\vec{B}(\vec{r})$ can be rewritten as

$$\vec{B}(\vec{r}) = \left\{ \frac{\mu_0}{4\pi} \cdot \frac{3\vec{n} \cdot \vec{m}}{r^3} \right\} \cdot \vec{n} - \left\{ \frac{\mu_0}{4\pi} \cdot \frac{1}{r^3} \right\} \cdot \vec{m} \qquad (2)$$

Because the expressions in the curled brackets of (2) are scalar quantities, it becomes obvious, that $\vec{m}$, $\vec{r}$ and $\vec{B}(\vec{r})$ are in a common plane.

1.3. Position of maximum Signal Strength

The magnitude of the magnetic flux density $B(r,\vartheta)$ generated by a magnetic dipole can be expressed by using equations given in [6] as

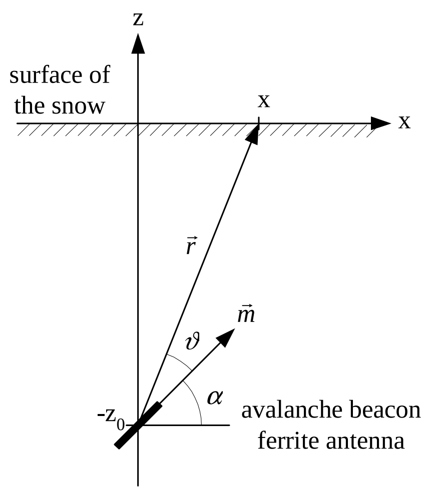

Figure 2
Definition of the variables for the calculation of the position of maximum field strength.

$$B(r,\vartheta) = \frac{\mu_0\, m}{4\pi} \cdot \frac{\sqrt{1 + 3\cos^2\vartheta}}{r^3}\,. \qquad (3)$$

In equation (3) *r* is the distance from the dipole and ϑ the angle between the magnetic dipole moment $\vec{m}$ and the direction of observation. The situation is shown in figure 2. Using the variables defined in figure 2, we get for the magnetic flux density at the surface of the snow as a function of *x*, if $\vec{m}$ lies within the xz – plane.

$$B(x) = \frac{\mu_0 m}{4\pi} \frac{\sqrt{1 + \frac{3 \cdot (x \cdot \cos\alpha + z_0 \sin\alpha)^2}{(x^2 + z_0^2)}}}{\sqrt{x^2 + z_0^2}^{\,3}} \qquad (4)$$

It is sufficient to look onto *x* only, since the magnetic field is symmetric with respect to the axis of the antenna. Adding a *y* component to the position on the snow surface will increase *r* and ϑ. Therefore the numerator of (3) will be decreased and the denominator will be increased, resulting in a smaller value for *B*.

Calculations of the signal level at the snow's surface using (4) allow to identify two critical situations: Figure 3 shows the first for a burying depth of 2m. There is a deviation of up to 50cm between the point on the surface directly above the victim and the location of maximum signal strength. The second occurs for an angle α of zero or 180 degrees. Here the maximum is very flat and the range of *x* for a decrease of only 0.1 dB with respect the maximum at $x = 0$ extends from -0.53m to 0.53m, also resulting in a large uncertainty.

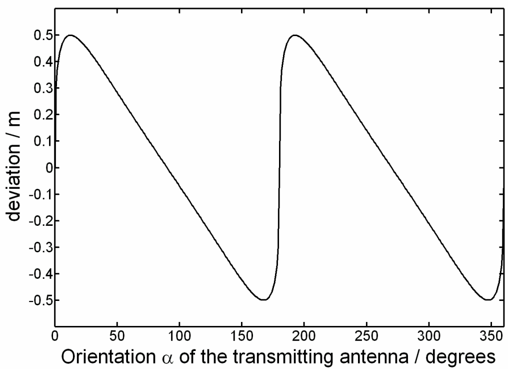

Figure 3
shows the deviation in meters of the position of the maximum signal level at the surface of the avalanche as a function of the orientation α of the transmitting avalanche beacon antenna, if the victim is buried 2 m below the surface. At angles of 0, 180 and 360 degrees the maximum signal level can be measured directly above the victim. However, for angles of about 15, 165, 195 and 345 degrees there is a deviation of 0.5 m. This is too much for starting to dig out the victim

2. DETERMINATION OF THE Z – COORDINATE OF THE VICTIM'S POSITION

If $\vec{r}_A$ denotes the position of the avalanche beacon, $\vec{r}_M$ the position of the receiving antenna, which measures the magnetic flux density $\vec{B}(\vec{r}_M)$, then the vector $\vec{B}(\vec{r}_M)\times(\vec{r}_M-\vec{r}_A)$ is perpendicular to the plane defined by $\vec{B}(\vec{r}_M)$ and $\vec{r}_M-\vec{r}_A$. Then for all points $\vec{x}$ on the plane we get [7]

$$\left[\vec{B}(\vec{r}_M)\times(\vec{r}_M-\vec{r}_A)\right]\cdot(\vec{x}-\vec{r}_A)=0 \qquad (5)$$

If we have three points of measurement $\vec{r}_{M1}$, $\vec{r}_{M2}$ and $\vec{r}_{M3}$ and the corresponding magnetic fields $\vec{B}_1=\vec{B}(\vec{r}_{M1})$, $\vec{B}_2=\vec{B}(\vec{r}_{M2})$ and $\vec{B}_3=\vec{B}(\vec{r}_{M3})$, respectively, then three planes are defined in this way.

$$\left[\vec{B}_i\times(\vec{r}_{M,i}-\vec{r}_A)\right]\cdot\vec{x}=\left[\vec{B}_i\times(\vec{r}_{M,i}-\vec{r}_A)\right]\cdot\vec{r}_A \qquad i=1,2,3 \qquad (6)$$

For three planes in general there will be exactly one common point, i.e. the system of equations (6) has a unique solution. In our case, however, the direction of $\vec{m}$ must lie in each of the three planes defined by (6). So there must be not only one point but an entire straight line, which is part of each plane. A necessary mathematical condition for that is, that the determinant of the coefficient matrix for the system of the three equations must vanish [7]. Since the determinant is invariant with respect to the mathematical operation of transposition [7], it can directly be written using the normal vectors of the planes.

$$\det\left(\vec{B}_1\times(\vec{r}_{M,1}-\vec{r}_A),\vec{B}_2\times(\vec{r}_{M,2}-\vec{r}_A),\vec{B}_3\times(\vec{r}_{M,3}-\vec{r}_A)\right)=0 \qquad (7)$$

Let $\vec{r}_A=(x_A,y_A,z_A)^T$ and assume, that the x_A and y_A coordinates of the victim's position are known, then (7) is a quadratic equation for the remaining z – coordinate, usually resulting in two solutions. Since the direction of the magnetic moment $\vec{m}$ of the ferrite antenna is defined by the common straight line of the three planes, it is possible to calculate $\cos^2\vartheta$ in equation (3) for each of the points of measurement and each solution of (7).

$$\cos^2\vartheta_i=\frac{\left[\pm\vec{n}_m\cdot\left(\vec{r}_{Mi}-(x_A,y_A,z_A)^T\right)\right]^2}{\left|\vec{r}_{Mi}-(x_A,y_A,z_A)^T\right|^2} \qquad i=1,2,3 \qquad (8)$$

Here $\vec{n}_m$ is a unit vector in the direction of $\vec{m}$ or $-\vec{m}$ defined by the common straight line of the three planes. With the aid of (8) and (3) the theoretical value of the ratio of the magnetic fields can be calculated for each of the two z_A – values.

$$a_{ij}=\frac{1+3\cos^2\vartheta_i}{1+3\cos^2\vartheta_j}\cdot\frac{\left|\vec{r}_{Mj}-(x_A,y_A,z_A)^T\right|^3}{\left|\vec{r}_{Mi}-(x_A,y_A,z_A)^T\right|^3}$$

$$i,j=1,2,3 \qquad i>j \qquad (9)$$

The values a_{ij} will be identical to $\left|\vec{B}_i\right|/\left|\vec{B}_j\right|$ only for one of the two z_A – values, which then is the correct one.

3. NEW SEARCH STRATEGY

3.1. General Description

According to the theoretical considerations above three measurement points would be sufficient. But when taking measurement errors into account, better confidence is obtained by using more. However, this increases the time for the calculations. Five points have proven to be a good compromise. After the avalanche victim has been localized by the standard search method, this position is marked. Subsequently five measurements of the magnetic flux density are performed resulting in the values $\vec{B}_1^*$, $\vec{B}_2^*$ . . . $\vec{B}_5^*$, respectively. The positions $\vec{r}_1^*$, $\vec{r}_2^*$ . . . $\vec{r}_5^*$ of the measurements should be located at a distance of 1 to 4m from the marked point and should have an approximately uniform angular distribution (fig. 4).

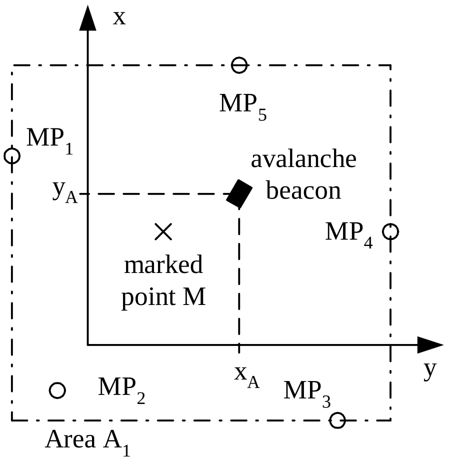

Figure 4
shows the positions of the measurement positions MP_1 to MP_5 around the initially marked point M determined by the standard search method. A_1 is the smallest rectangular area with sides parallel to the axes, which contains all points.

Using the minimum and maximum x and y values of the measurement positions a rectangular area A_1 can be defined, which certainly includes the true horizontal position (x_A, y_A) of the avalanche beacon. On A_1 a coarse quadratic grid is defined. For any triple of measurement points and corresponding magnetic flux values and for any xy - coordinates of the grid two z_A - values can be calculated according to equation (7). Using (8) and (9) the theoretical ratio α_{ij} of the magnetic flux densities for any pair of measurement points can be calculated. The optimum point of the grid and z_A – value is determined by minimizing the following expression

$$E = \sum_{\substack{i,j=1 \\ i \neq j}}^{5} \left(\alpha_{ij} - \frac{\left|\vec{B}_i^*\right|}{\left|\vec{B}_j^*\right|} \right)^2 . \qquad (10)$$

Using a smaller area A_2 around the first optimum point together with a finer grid allows to find a better solution with a resolution limited by the grid size. This can be repeated, if necessary.

3.2. Simulation Results

Simulations of the localization procedure described above have been performed in order to see, how sensitive the result depends on the choice of the measurement positions MP_1 to MP_5 and possible measurement errors for the magnetic field. MP_1 to MP_5 have been determined in the following manner. The starting point was a circle of 6m diameter in the xy - plane with its centre located at a z – coordinate z_0 directly above the avalanche beacon. Then five points on this circle generating a regular pentagon have been chosen. To get the final positions for the measurements each coordinate of the five points was changed by adding a random value uniformly distributed in the range from $-\Delta x_{\max}$ to $+\Delta x_{\max}$, $-\Delta y_{\max}$ to $+\Delta y_{\max}$ and $-\Delta z_{\max}$ to $+\Delta z_{\max}$, respectively. In order to include measurement errors in the simulation, additionally each component of the five B – vectors was changed in a similar manner by adding a randomly distributed error. The random distribution was a normal distribution with mean 0 and a standard deviation of $p \cdot \left|\vec{B}_i^*\right|$, $0 \le p < 1$. The orientation of the magnetic moment of the avalanche beacon's ferrite antenna was completely random, too. All the random values described above changed from simulation to simulation. Three grid sizes were used: 20cm for A1 , 5cm for A_2 and 2cm for A_3. The simulation results show, that the x and y coordinate of the avalanche beacon can be determined much better than the depth. The results are shown in figure 5.

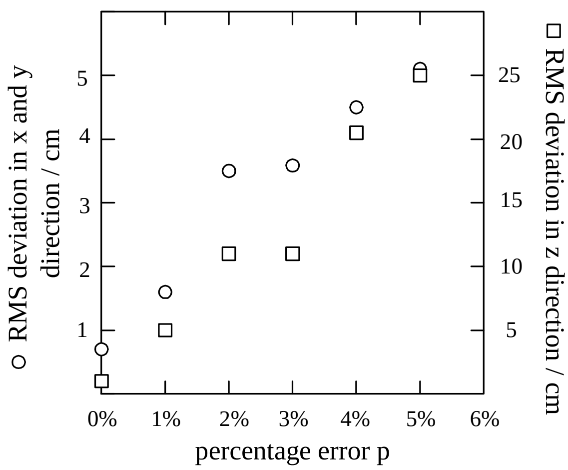

Figure 5
shows the RMS deviations for 20 simulations for each percentage error p. The circles indicate the average of the deviations in x and y direction, the squares those in z. Note, that the scales for both types of deviations differ by a factor of 5.

In case of errors for the B - field the localization algorithm as described above sometimes fails, because the errors may lead to a better optimum at a wrong position. In order to avoid such results, three additional checks are performed: Equation (7) must have a real (not imaginary) solution, acceptable z – values must be below the plane defined by $\vec{r}_{M1}$, $\vec{r}_{M2}$ and $\vec{r}_{M3}$ and the signal level generated at all points of measurement must be compatible with the limits for the magnetic moment of the transmitting antenna as defined by the standard [4]. The simulations also clearly show, that the value of *E* cannot be used as a criterion for the precision of the localization.

4. EXPERIMENTAL RESULTS

Today's avalanche beacons – often known by the French acronym ARVA (Appareil de Recherche de Victimes d'Avalanche) – are based on transmitter devices generating a pulsed magnetic field at $457kHz \pm 80Hz$, with a pulse period of $1000 \pm 300ms$ and a duty cycle of 70ms to 900ms. Its exact specifications are regulated by the standard ETS 300718 [4] for ensuring compatibility between different brands and models. For applying the new search algorithm it is necessary to detect the active parts of the beacon signal and hence to estimate the related magnetic field vectors $\vec{B}_i$ at different MPs.

Figure 6 depicts the experimental setup, which was developed for testing the new search algorithm. One of the main components of the test system is the ferrite core of the 3D – antenna, as shown in Fig. 7. The material of the rods is 3B1 from Ferroxcube with an initial permeability of 900 ± 20 and a saturation magnetization of 380 mT [8]. For reducing antenna coupling between the three different axes the rods have to be strictly orthogonal with respect to one another.

In addition, the coils on each antenna have to be electrically shielded, since the electronic oscillator of the avalanche beacon also generates an electric field, which could disturb the magnetic field measurements significantly. The 3 antenna amplifiers are based on a modified version of the amplifier described in [9], which is running in resonant mode. The sampled output signals $v_X(k)$, $v_Y(k)$ and $v_Z(k)$ of the amplifiers were captured using a USB powered four channel 12 bit resolution digital oscilloscope. The capture time at each MP was chosen to be 2s at a sampling rate of 1MSamples/s. The complete analysis was developed in MATLAB running on a ruggedized laptop. For the analysis of the capture buffers $v_X(k)$, $v_Y(k)$ and $v_Z(k)$ it was necessary in a first step to suppress unwanted interference by applying a band pass filter. with start and stop frequencies of $457kHz \pm 100Hz$, respectively. The detection and estimation of the magnetic field vectors $\vec{B}_i$ was in a second step based on a matched filter $h(k)$ [11]

$$\begin{aligned} &\varphi_X(k) = v_X(k) * h(k) \\ &\varphi_Y(k) = v_Y(k) * h(k) \\ \text{and}\quad &\varphi_Z(k) = v_Z(k) * h(k), \end{aligned} \tag{11}$$

where $h(k) = s(-k)$ is the matched filter with respect to the transmitted beacon signal $s(k)$ as defined in the standard. The maxima of the matched filter outputs are for the signal detection compared against a SNR threshold γ

Figure 6
shows the experimental setup. At the top there is the 3D ferrite antenna, then follows the unit containing the electronic compass, the pressure sensor and the local display. In the box on the rear side there are the PicoScope, type 3424 and the antenna amplifiers connected to the laptop at the bottom.

Figure 7
Ferrite core of the 3 D antenna. The length of the three rods is approximately 110 mm.

$$\max_{\tilde{k}} \left\{ \left|\varphi_X(\tilde{k})\right|, \left|\varphi_Y(\tilde{k})\right|, \left|\varphi_Z(\tilde{k})\right| \right\} \geq \gamma\,, \tag{12}$$

which is the minimum SNR required for the further analysis. If none of the matched filter outputs $v_X(k)$, $v_Y(k)$ or $v_Z(k)$ fulfilled the SNR requirement, the MP was withdrawn and the current measurement had to be repeated at an additional MP. Otherwise $k_0 = \arg\max_{\tilde{k}} \left\{ \left|\varphi_X(\tilde{k})\right|, \left|\varphi_Y(\tilde{k})\right|, \left|\varphi_Z(\tilde{k})\right| \right\}$, the maximum position of the strongest matched filter output, was used for the estimation of the magnetic field components:

$$\vec{B}_i = a_0 \cdot \begin{pmatrix} \operatorname{sgn}(\varphi_X(k_0)) \cdot \sqrt{|\varphi_X(k_0)|} \\ \operatorname{sgn}(\varphi_Y(k_0)) \cdot \sqrt{|\varphi_Y(k_0)|} \\ \operatorname{sgn}(\varphi_Z(k_0)) \cdot \sqrt{|\varphi_Z(k_0)|} \end{pmatrix}, \qquad (13)$$

where a_0 is a scaling factor comprising the antenna, the amplifier and the data capturing properties. These magnetic field vectors were used for the further search strategy as described in section 3. Figure 8 exemplarily shows the graphical user interface depicting the results of the search algorithm.

5. CONCLUSION

We have shown by simulation and first experiments, that by using the properties of the magnetic field generated by an avalanche beacon it is possible to localize it with a precision, which is sufficient to immediately start to dig out the victim. So the time consuming step of mechanical probing is not necessary any more and the chance for survival becomes higher. However, for real use it is necessary to get the coordinates of the measurement points with the necessary precision automatically. This can be achieved by a differential GNSS system, which will be added as next step.

6. ACKNOWLEDGEMENTS

The work was supported by the German Federal Ministry of Research and Technology across the Raumfahrtagentur des Deutschen Zentrums für Luft- und Raumfahrt e.V., project number 50NA0702. The authors like to acknowledge the help of two student groups of the University of Applied Sciences Rosenheim during the academic years 2007/08 and 2008/09, who developed the hardware and the software for data capturing. The first group consisted of G. Astner, C. Dörrer , N. Engelmayer, B. Mehlhorn, M. Pretl, F. Sedlmeier, L. Tomanek, H. Willmann and S. Wurm. Members of the second group were M. Frisch, H. Gröll, M. Hogger, A. Hundhammer, B. Kaindl, S. Nagel, J. Schönhuber, H. Westermayer and L. Zenz.

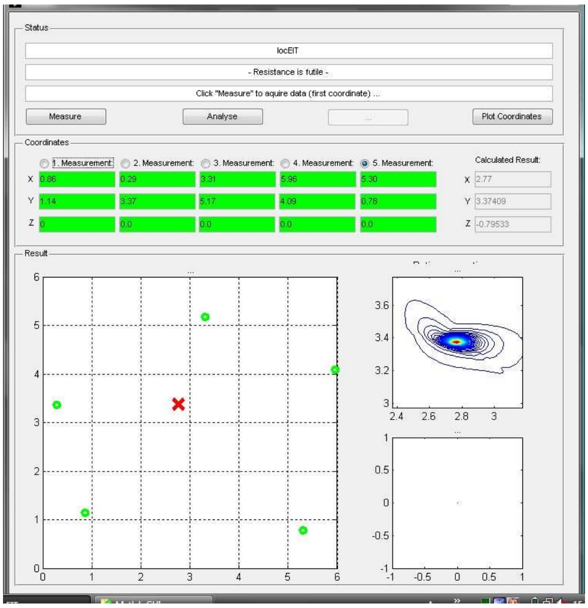

Figure 8

MATLAB graphical user interface implemented on the laptop. The coordinates of the measurement points can be seen in the table named "coordinates" in the upper half. On the right hand side the calculated coordinates of the avalanche beacon are displayed. The large square contains a graphical representation of these data. The circles represent the measurement points, the cross indicates the calculated position. The upper little square on the right hand side is a graphical display of the error as function of the coordinates. In this case the true position of the avalanche beacon was x = 2,80m, y = 3,36m and z = -0,71m. The errors in the x, y and z - directions were 3.0cm, -1.4 cm and 8.5cm, respectively.

7. REFERENCES

[1] M. Falk, M. Brugger and L. Adler-Kastner, "Avalanche Survival Chances", Nature, vol. 368, no. 1, p.21, 1994

[2] C. Semmel, D. Stopper, "LVS – Gerätetest", Panorama, Mitteilungen des Deutschen Alpenvereins, pp. 88-91, April 2007

[3] A. Dick, "Fühlen und Finden", Alpin, pp. 72 – 73, 2 / 2007

[4] ETSI Standard EN 300 718 – 1, V 1.2.1 (2001 - 05)

[5] J. D. Jackson, Classical Electrodynamics, 2'nd ed., John Wiley & Sons, Inc., New York, 2001

[6] Eugen Philippow, Grundlagen der Elektrotechnik, Verlag Technik, Berlin, 1992

[7] J. Heinhold, B. Riedmüller, Lineare Algebra und Analytische Geometrie, 2'nd ed., Carl Hanser Verlag, München, 1975

[8] Datasheet Ferrite 3B1, Ferroxcube www.ferroxcube.com/prod/assets/**3b1**.pdf

[9] D. Burchard, "Aktive Empfangsantenne, Überlegungen, Berechnungen und Versuche", UKW Berichte, pp. 235 – 249, 4 / 1994

[10] Ayuso et al., "Avalanche Beacon Magnetic Field Calculations for Rescue Techniques Improvement", Geoscience and Remote Sensing Symposium, pp. 722 – 725, IGARSS 2007

[11] J. Proakis, Digital Communication, McGraw - Hill Science, New York, 2000